Proceedings of the Twenty-first (2011) International Offshore and Polar Engineering Conference
Maui, Hawaii, USA, June 19-24, 2011

ISBN 978-1-880653-96-8 (Set); ISSN 1098-6189 (Set); www.isope.org

Numerical Simulation of an Oscillating Water Column Wave Energy Converter: Comparison of two Numerical Codes

J. M. Paixão Conde
Faculdade de Ciências e Tecnologia, Universidade Nova de Lisboa, Monte de Caparica, Portugal;
IDMEC, Instituto Superior Técnico, Universidade Técnica de Lisboa, Lisbon, Portugal

P. R. F. Teixeira
Universidade Federal do Rio Grande, Rio Grande, RS, Brazil

E. Didier
Laboratório Nacional de Engenharia Civil, Lisbon, Portugal;
MARETEC, Instituto Superior Técnico, Universidade Técnica de Lisboa, Lisbon, Portugal

ABSTRACT

This paper presents the results from the application of two numerical codes in the simulation of an oscillating water column wave energy converter. One of the codes (FLUINCO) is based on the finite elements technique, while the other (FLUENT) is based on the finite volume technique. The objective of this work is the validation of these codes for this type of flow, aiming the systematic application to wave energy converters design. The simulated case, corresponding to a simplified model tested experimentally, allows us to conclude that the numerical results have good quality, showing good correspondence between experimental and numerical results.

KEY WORDS: Wave Energy, Oscillating Water Column, Numerical Simulation, FLUINCO, FLUENT, RANS.

INTRODUCTION

The power associated with waves that reach all coastal areas of the world is estimated at approximately 10^{12} W. If this energy is captured in the open sea, without the losses associated to friction and breaking waves, this figure is estimated to be an order of magnitude higher (~10^{13} W), an amount comparable to the current energy consumption in the world (Falnes, 2002; Panicker, 1976). Although this amount is only a small portion of the potential of wind and solar, the potential for large scale use of energy from ocean waves has the ability to cover a substantial portion of electricity consumption worldwide.

The use of wave energy along the coastal areas is a particularly attractive option in high-latitude regions. Along the coasts of northern Europe, North America, New Zealand, Chile and Argentina, for instance, are found high densities of annual average wave energy (typically between 40 and 100 kW per m of wave front) (Pontes and Falcão, 2001).

Based on various energy extracting methods, a wide variety of systems has been proposed, but only a few full-sized prototypes have been built and deployed in open coastal waters and connected to the electric grid.

The Oscillating Water Column (OWC) is considered to be one of the more technically known Ocean Wave Energy Converter (OWEC), due to the large research effort that has been subject in recent years. This device is also one of the first to have reached the status of full-sized prototype deployed in the real sea.

An OWC-OWEC consists of a partially submerged structure, open below the water free surface, within this structure is trapped an air pocket above the free surface. The oscillating movement of the free surface inside the pneumatic chamber, produced by the incident waves, forces the air to flow through the turbine which is directly coupled to electrical generator (Falnes, 2002). The closer to the natural frequency of the water column are the frequencies of the waves, the greater the energy output.

Most of the first prototypes were installed in the shoreline, or in breakwaters, in different parts of the world (e.g.: Toftestallen, Norway, 1985; Sakata, Japan, 1988; Trivandrum, India, 1990; Pico, Portugal, 1999; Limpet, Scotland, 2000; Port Kembla, Australia 2005).

Although the coastal systems have the advantages of the ease of access and lack of moorings, they have the disadvantage of having lower incident energy, compared with the available offshore, due to dissipative effects of the wave breaking and the seabed friction. The evolution from coastal systems to offshore systems, where the wave energy is higher, is advantageous because the latter are not constrained by the morphology of the coast, or subject to tidal effects.

Some floating OWC systems have already been developed, e.g.: Migthy Whale (Japan), Energetech (Australia), OE buoy (Ireland), Sperboy (England). In the medium to long term, it is expected the installation of floating offshore OWC-OWEC's farms, in areas with depths of 40 to 70 m (Clément et al., 2002).

The chain of energy conversion in the OWC-OWEC consists of: conversion of wave energy to pneumatic energy in the OWC's pneumatic chamber; conversion of pneumatic energy to mechanical energy at the turbine shaft; and conversion to electrical energy in the alternator.

It is not common practice to use a single numerical code to simulate all

the effects verified in this type of device. This code should accurately simulate the 3D wave propagation and its transformation when subjected to the OWC-OWEC influence; the water inflow and outflow in the device; the air flow in the pneumatic chamber and the damping caused by the pressure loss at the turbine. A correct simulation of these flows is essential to evaluate the design of the pneumatic chamber and to determine the operating conditions of the turbine (Paixão Conde and Gato, 2008).

An OWC-OWEC in the form of a vertical tube of small circular cross-section is a geometrically simple point absorber that has been studied analytically and experimentally by many authors.

Evans (1978) simulated the water free surface by the motion of a rigid piston without mass for the case of a vertical tube of small diameter in relation to the wavelength. In this theoretical model, the Power Take-off (PTO) is simulated by a linear mass-spring-damper. Falcão and Sarmento (1980) and Evans (1982) considered an oscillating free surface with uniform pressure distribution. The instantaneous PTO power is the product of volumetric flow rate displaced by the free surface and the internal air pressure in the pneumatic chamber. Other authors have used codes based on the Boundary Element Method (e.g. Lee et al., 1996; Brito and Melo, 2000; Delauré and Lewis, 2003; Lopes et al. 2007).

The study of this type of problem is closer to the reality, if we use a model that considers the complete Navier-Stokes (N-S) equations in the numerical simulations. This paper presents a comparison of numerical results, obtained by two N-S solvers, in the simulation of the action of regular waves on a simplified OWC-OWEC model tested in a wave flume (Lopes et al., 2007). One of the numerical codes, FLUINCO (Teixeira and Awruch, 2000; Teixeira, 2001), uses a finite element method to solve the N-S equations and considers the water free-surface as a boundary where the atmospheric pressure is applied. The other code, FLUENT, uses a finite-volume method to solve the N-S equations and captures the water free-surface using the Volume of Fluid (VoF) approach. The objective of this work is the validation of these codes for this type of flow, aiming the systematic application to wave energy converters design.

NUMERICAL CODES

Code FLUINCO

The code FLUINCO (Teixeira and Awruch, 2000; Teixeira, 2001) uses a fractionated method to simulate free surface 3D incompressible fluid flow problems. It employs the semi implicit, two steps, Taylor-Galerkin method to discretize the N-S equations in space and in time.

For the space discretization the classical Galerkin weighted residuals method, using a tetrahedral element, is applied. The tetrahedral element has the advantage to be easily adapted to areas of complex geometry and to be a good computational efficiency element.

An Arbitrary Lagrangian Eulerian (ALE) formulation is used to allow the solution of problems involving large relative motion between bodies and surfaces and the motions of the free surface.

The model considers the free surface subjected to a constant atmospheric pressure (usually the reference value is zero) and imposes the free surface kinematic boundary condition, using the ALE formulation (Ramaswamy and Kawahara, 1987).

The spatial distribution of the mesh velocity is such that the distortion of elements is minimized by its smoothing using functions that weigh the influence of the speed of each node belonging to the boundary surfaces.

The turbulence is modelled with a turbulent viscosity, defined by Mittal and Tezduyar (1995), and a mixing length, defined by Johns (1991).

Other details of the application of this code to this type of problems may be found in Teixeira et al. (2009).

Code FLUENT

The code FLUENT (version 6.3.26) applies a finite volume technique to solve the continuity and the N-S equations. In this code the variables are defined in the center of each element. The diffusive terms of the equations are discretized by the second order central difference scheme. There are available: different interpolation schemes for the convective terms (first order Upwind, first order power law, second order Upwind, MUSCL and QUICK); different resolution algorithms (Coupled, SIMPLE, SIMPLEC and PISO); and different turbulence models (Fluent, 2006).

The capture of the free surface is done by the VOF method. This method, originally developed by Hirt and Nichols (1981) identifies the position of the free surface from a scalar indicator, the volume fraction, which takes the value 0 in the air and 1 in the water. The position of the free surface is arbitrarily defined by the value 0.5.

In the simulations carried out were used: the 3D module of the code; the implicit formulation; the 2nd order time discretization; and the standard k-ε turbulence model. In the resolution of the system of equations was used the SIMPLEC algorithm with under relaxation, only in the equations of k and ε, with the coefficients equal to 0.8. The convective terms in the faces of the control volumes, for the components of momentum, k and ε are determined by the 2nd order Upwind scheme. The volume fraction on the faces of control volumes is determined by a modified version of the High Resolution Interface Capturing (HRIC) scheme (Peric and Ferzinger, 1997). The pressure is determined by the PRESTO! (PREssure STaggering Option) scheme.

CASE DESCRIPTION AND SIMULATION CONDITIONS

In this paper we intend to reproduce one of the experimental tests described by Lopes et al. (2007). Fig. 1a shows one of these tests carried out with the prototype in the wave flume at the Department of Architecture and Civil Engineering at Instituto Superior Técnico (IST), Lisbon, Portugal. This flume is 20 m long and 0.70 m wide.

The simplified physical model of OWC-OWEC consists of a small vertical hollow cylinder open at the ends and placed vertically (Fig. 1b). Its axis is coincident with the longitudinal symmetry plane of the flume and is placed 9 m from the wave generator. The cylinder has an inner radius ($r=d/2$) and a thickness (t) equal to 0.025 m and 0.0025 m, respectively. The water depth at rest (D) and wave amplitude (a) are equal to 0.4 m and 0.015 m, respectively.

In the experimental study were considered: different submergence lengths (s), respectively, 0.1 m, 0.18 m and 0.245 m; different frequencies (f) in the range of 0.5~1.6 Hz; and were made tests with the top of the cylinder open to the atmosphere and with a pressure loss. In this study were considered only the tests without pressure loss and with s = 0.18 m.

In the frequency range considered the ratio D/L (where L is the wavelength) is comprised between 0.11 and 0.66. Only for frequencies above 1.4 Hz the incident waves are in deep water condition ($D/L>0.5$), the remaining are in intermediate depth ($0.5>D/L>0.05$) (LeMéhauté, 1976).

Although the ratio of outside diameter of the cylinder by the width of the channel is small (~ 7.9%), the experiments do not reflect the effect of a single stand alone device in the open sea, but of an infinite number of devices side by side perpendicularly to the incident waves, because the flume walls act as planes of symmetry.

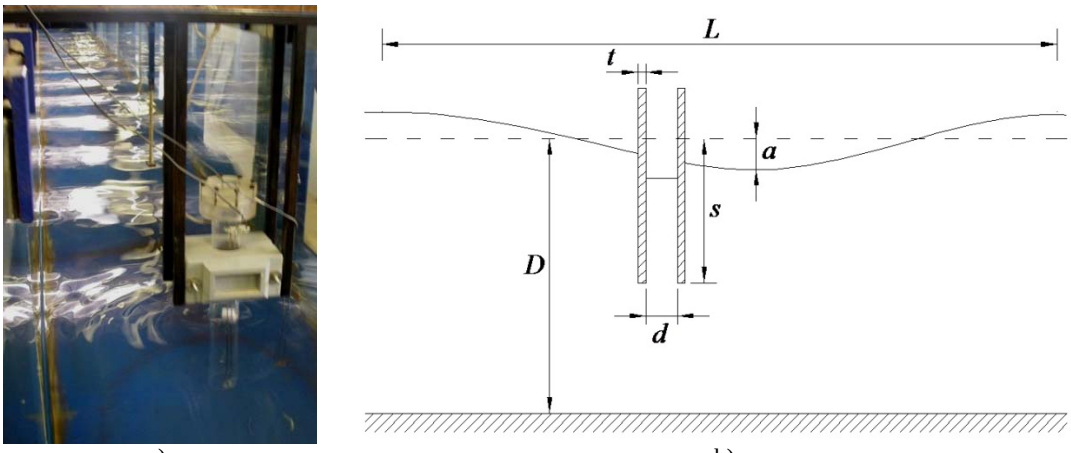

a) b)

Fig. 1: a) Physical model tests (Lopes et al, 2007); b) Variables definition scheme.

The flow regime due to wave-structure interaction can be better understood by the calculation of the Keulegan-Carpenter number, $KC = u\,T/d_e$, where u is the amplitude of the maximum velocity of the flow (in this case the wave speed at the surface), T is the wave period and d_e is the outer diameter of the cylinder. The values of KC for the cases studied were between 1.7 and 2.9. In this range of KC, the inertia forces are predominant compared to the drag ($KC < 3$ to a vertical circular cylinder submerged to the bottom).

The ratio d_e/L is another parameter used to analyze the wave-structure interaction. For the cases studied, this ratio varies from 0.015 to 0.09, with higher values referring to waves of higher frequencies. Note that the higher this ratio, the greater the diffraction effect on the wave transformation (it is considered that to $d_e/L < 0.2$, the effects of diffraction can be neglected). It is noteworthy that in the present work, the cylinder is partially submerged, which differs from the cases studied by several authors who have established limits for these flow parameters. Furthermore, the cylinder is hollow, which means that an interaction between the mass of fluid inside the cylinder and the external flow exists.

It was found (Paixão Conde and Didier, 2009; Teixeira et al., 2009) the presence of turbulence in the region near the submerged end of the cylinder, which is the main reason for the use of turbulence models.

Taking advantage of the symmetry of the problem in relation to the longitudinal and vertical planes, the computational domain is only half the actual domain ($0 \le y \le 0.35$ m) in the simulations carried out with both codes.

Code FLUINCO

In the simulations carried out with the numerical code FLUINCO the channel is 5.5 m long and the axis of the cylinder is 2.0 m from the wave generator.

The finite element mesh has 121,420 nodes and 664,383 tetrahedra (Fig. 2a). The elements' edge average size in the upstream region from the cylinder is approximately 0.02 m. In the region nearby to the cylinder, was used an element's edge average size of 0.002 m, equivalent to 40 divisions of the inner circumference of the cylinder. The time step adopted was 0.0002 s, this value satisfies the Courant limit, i. e., $V\,\Delta t/\Delta x < C$, with $C = 0.25$. The value of Δt is obtained to each element, being chosen for the entire domain the smallest among them (Teixeira, 2001).

The monochromatic wave is generated by the direct imposition of the surface elevation and horizontal and vertical components of the velocity. These values are determined from the profiles of velocity and position of the free surface obtained from the linear theory of waves.

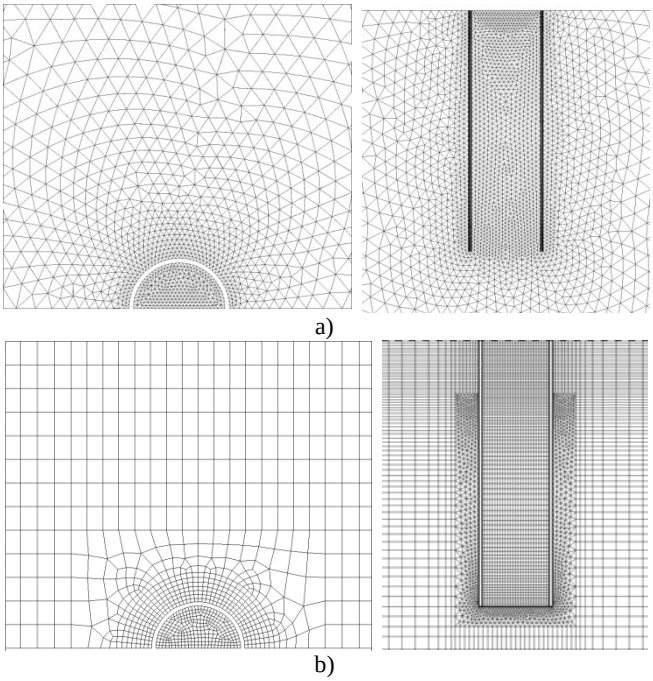

a)

b)

Fig. 2 Details of the discretization mesh: a) FLUINCO; b) FLUENT.

Code FLUENT

In the simulations performed with code FLUENT the cylinder axis is at position $x = y = 0$ and the free surface is at rest at position $z = 0$. The numerical flume extends only to $x/L \approx -1$ in the wave generator direction and until $x/L \approx 4$ in the opposite direction. In the vertical direction the domain is comprised between $-0.4\text{ m} \le z \le 0.07$ m. The cylinder extends from z = -0.18 m (in the water) to the upper boundary (in the air).

The mesh discretization used is composed of approximately 4.9×10^5 control volumes for the higher frequency and 6.8×10^5 control volumes for the lower frequency, being more refined in the vicinity of the cylinder (Fig. 2b).

The perimeter of cylinder semi-circumference is discretized by 40 segments. In the wave propagation region, $-0.02\text{ m} \le z \le 0.02$ m, the discretization consists of 24 equal segments, i. e., 18 segments by wave height. From $x/L = -1$ until $x/L = 1$ are used approximately 60 segments by wavelength. From $x/L = 1$ until $x/L=4$ (wave dissipation zone) the length of the segments is progressively increased until reaching ~0.35L.

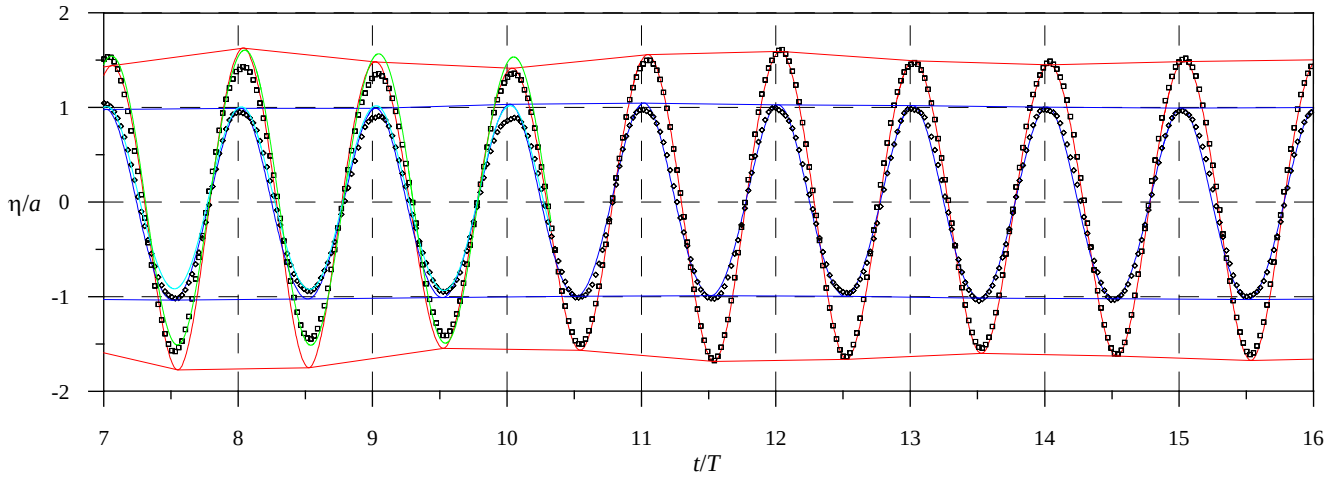

Fig. 3 Comparison of the free-surface elevation time-series, inside and outside of the cylinder, obtained by the two numerical codes, with the corresponding experimental data (Lopes et al., 2007), for f = 0.9 Hz. FLUINCO (— interior probe; — exterior probe), FLUENT (— interior probe; — exterior probe) and experimental (◇ interior probe; □ exterior probe)

The initial conditions imposed were: the components of the velocity equal to zero in the entire domain; and the hydrostatic pressure equal to zero at the free surface. The monochromatic wave was generated in the vertical boundary with $x = -L$ by the direct imposition of the surface elevation and velocity components. These conditions were written on a User Defined Function (Fluent, 2006) based on the velocity profiles and position of the free surface obtained from the linear theory of waves.

At the bottom of the flume, on the opposite wall to the wave generator and on the cylinder walls the adherence condition was used with zero velocity. In the upper boundary is imposed the atmospheric pressure, allowing the entry or exit of the air. The time step used was $T/640$. A maximum of five iterations per time step was imposed, this value is sufficient to reduce all residues to values lower than 10^{-3} (Barreiro et al., 2009).

RESULTS AND DISCUSSION

Firstly we analyze the 0.9 Hz regular incident wave case. Figure 3 shows the water free-surface elevation time-series for two probes placed in the transversal plane coincident with the axis of the cylinder: one is located inside cylinder (in the axis) and the other is outside in an intermediate position between the flume wall and the cylinder.

It was found that is necessary approximately 10 periods of wave for the evolution of the free surface measured at the two probes to stabilize. After stabilization, it is observed that the numerical results are in good agreement among themselves and with experimental data.

Although not graphically presented in this paper, it was found that for this frequency, there are high velocity gradients and asymmetry in the flow near of the lower opening of the cylinder (Paixão Conde and Didier, 2010; Teixeira et al., 2009). Despite this fact, there is a uniform flow towards the free surface, which contributes to the horizontal shape that it acquires throughout the entire period. This behavior has become clear, either by graphical representation of the free surface in several instants, either by free surface probes placed at various locations inside the cylinder. Lopes et al. (2007) achieved the same effect by numerical simulation using of the commercial boundary elements program WAMIT (2004).

Figs. 4c~4l present the comparisons of the free surface elevation time-series inside and outside of the cylinder, obtained by the two numerical codes, in the frequency range 0.6~1.5 Hz. Figs. 4a~4b show only the simulations with the FLUENT code. These figures also show the envelopes of the free surface elevation, inside and outside of the cylinder, obtained by the FLUENT code.

For the frequencies 0.5 Hz and 0.55 Hz the appearance of a second frequency inside of the cylinder on the downward phase was found. This effect is responsible for the changing of behavior of the amplification factor and phase angle (Fig. 5). Lopes et al. (2007) observed a similar effect for the frequency 0.6 Hz. For remaining the frequencies a similar behavior in the simulations obtained by the two numerical codes is observed.

From the results presented in Figs. 3~4 is possible to estimate the amplification factor, Q, ratio between the maximum elevation measured inside and outside of the cylinder, and the phase angle, θ, angular difference between the waves measured outside and inside of the cylinder. Fig. 5 shows the comparison of the values obtained numerically with the experimental ones for frequencies from 0.5 Hz to 1.6 Hz. For the amplification factor, apart from the frequency range 0.5~0.6 Hz, the agreement between numerical and experimental results is good.

For a cylinder of small diameter in comparison with its submergence length (s), 0.18 m for studied case, resonance occurs at a frequency $f = \sqrt{g/s}$, where g is the gravitational acceleration, resulting f = 7.382 rad/s = 1.17 Hz.

It can be observed on Fig. 5 that the resonant frequency found in both experimental tests and in numerical simulations was around 1.1 Hz, near to the theoretical value.

For the phase angle (θ): there is a good concordance between numerical and experimental results on the range 0.7~0.9 Hz; there is a difference between the behavior observed for the FLUENT results on range 0.5~0.6 Hz and FLUINCO and experimental results, which is consistent with that seen in Figs. 4a and 4b; in the transition region around the resonance frequency (0.9~1.3 Hz) both numerical codes tend to overestimate the phase shift; in the frequency range 1.3~1.6 Hz FLUINCO obtains closer results to the experimental than FLUENT, which tends to overestimate the phase shift.

CONCLUSIONS

This paper presented the results from the application of two numerical codes in the simulation of a OWC-OWEC. One of the codes (FLUINCO) is based on finite elements technique, while the other (FLUENT) is based on finite volume technique. The aim of the study was to validate these codes for this type of flow, in order to apply them systematically to wave energy converters design.

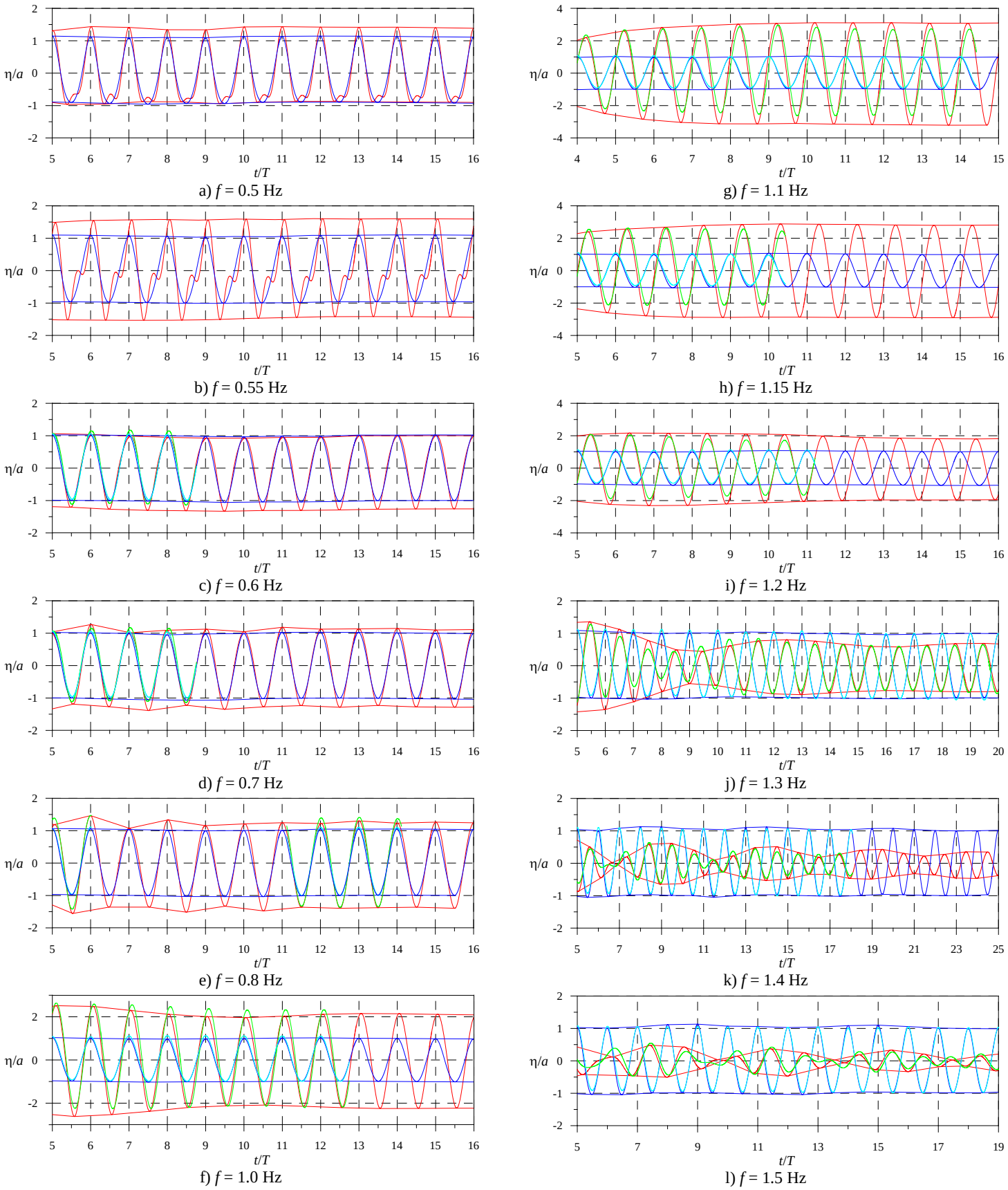

a) f = 0.5 Hz
b) f = 0.55 Hz
c) f = 0.6 Hz
d) f = 0.7 Hz
e) f = 0.8 Hz
f) f = 1.0 Hz
g) f = 1.1 Hz
h) f = 1.15 Hz
i) f = 1.2 Hz
j) f = 1.3 Hz
k) f = 1.4 Hz
l) f = 1.5 Hz

Fig. 4 Comparison of the free-surface elevation time-series, inside and outside of the cylinder, obtained by the two numerical codes. FLUINCO (— interior probe; — exterior probe), FLUENT (— interior probe; — exterior probe).

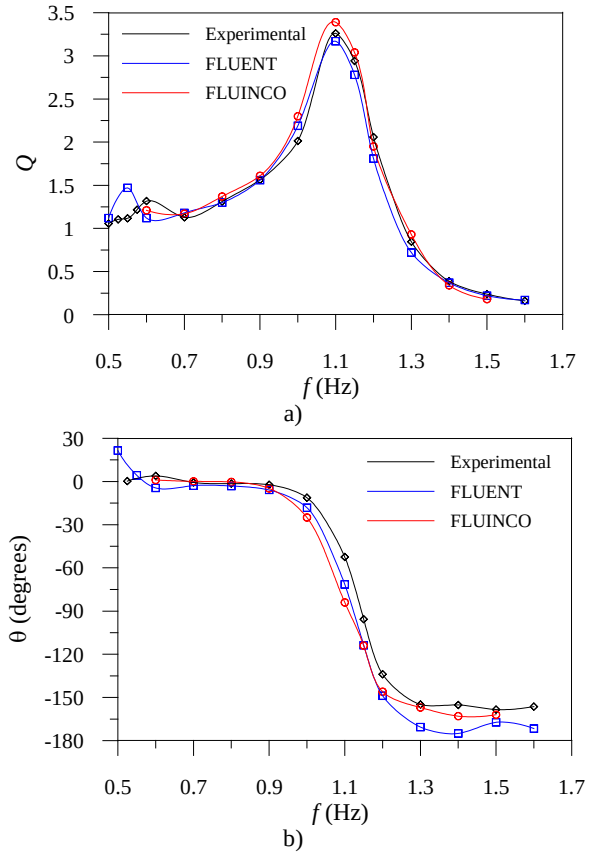

Fig. 5 Amplification factor, Q, and phase angle, θ, of the response depending of the incident wave frequency.

The simulated case corresponds to a simplified model of an OWC-OWEC tested experimentally in a channel with 0.4 m deep and 0.70 m wide. The model is a hollow cylinder with inner diameter of 0.05 m and thickness of 0.0025 m. It was placed in the plane of symmetry of the channel and its submerged part was 0.18 m from the free surface at rest. Monochromatic incident waves with 0.015 m in height and different frequencies in the range 0.5~1.6 Hz were simulated.

It was made a detailed analysis of the 0.9 Hz frequency case, comparing the elevations inside and outside of the cylinder with the experimental data, obtaining good agreement. It was found in this case, that the flow undergoes strong perturbations around the submerged end of the cylinder, but it stabilizes as it approaches the free surface. That is why the free surface inside the cylinder remains nearly flat and horizontal during the simulation.

The other simulations were performed varying the incident wave frequency, which enabled an analysis of the amplification factor and phase angle between the free surface elevations inside and outside the cylinder. The numerical results showed a behavior very similar to the experiments where was observed a maximum elevation in the interior of cylinder around the frequency of 1.1 Hz, also predicted by theoretical analysis.

The analysis made in this study show the phenomena that occur in the interactions between an OWC-OWEC (vertical cylinder) and monochromatic waves, considering the full Navier-Stokes equations, where the viscosity and turbulence effects are included.

Although the two numerical codes use different numerical techniques: finite element and finite volume; capture the free surface (VOF technique) and follow up of the free surface (kinematic boundary condition of the free surface); and the discretization meshes use different elements, hexahedrons and tetrahedra, we obtain very similar results.

The simulations were performed for a case in which the free surface is subjected to a constant pressure equal to the atmospheric pressure. In a real practical case there will be, inside of the pneumatic chamber, a pressure value different from the atmospheric due to the effect of the turbine. Taking this into account, in future work, simulations will be carried out including this effect.

ACKNOWLEDGEMENTS

The authors acknowledge the funding of research centers IDMEC and MARETEC. The authors also gratefully acknowledge M.F.P. Lopes for supplying his experimental data.

REFERENCES

Barreiro, T, Didier, E, Gil, L, and Alves, M (2009). "Numerical Simulation of the Nonlinear Flow Generated by the Interaction Between Waves and Punctual Wave Energy Converters", in Portuguese, *Proc. III National Conference in Fluid Mechanics, Thermodynamics and Energy*, Bragança, Portugal.

Brito-Melo, A (2000). *Modeling and pre-dimensioning of oscillating water column power plants: application to the Pico (Azores) wave power plant*, in Portuguese, PhD Thesis, Instituto Superior Técnico (Lisbon)/École Centrale de Nantes.

Clément, A, Mccullen, P, Falcão, AFO, Fiorentino, A, Gardner, F, Hammarlund, K, Lemonis, G, Lewis, T, Nielsen, K, Petroncini, S, Pontes, MT, Schild, P, Sjöström, B-O, Sorensen, HC, and Thorpe, T (2002). "Wave Energy in Europe: Current Statues and Perspectives", *Renewable and Sustainable Energy Reviews*, Vol 6, pp 405-431.

Delauré, YMC, and Lewis, A (2003). "3D hydrodynamic modeling of fixed oscillating water column wave power plant by a boundary element methods", *Ocean Engineering*, Vol 30, pp 309-330.

Evans, DV (1978). "The oscillating water column wave-energy device", *Journal of the Institute of Mathematics and Applications*, Vol 22, pp 423-433.

Evans, DV (1982). "Wave-power absorption by systems of oscillating surface pressure distributions", *Journal of Fluid Mechanics*, Vol 114, pp 481-499.

Evans DV, Porter, R (1996). "Hydrodynamic characteristics of an oscillating water column device", *Applied Ocean Research*, Vol 17, pp 115-164.

Falcão, AFO, Sarmento, AJNA (1980). "Wave generation by a periodic surface pressure and its application in wave-energy extraction", Proc *15th Int. Cong. Theor. Appl. Mech.*, Toronto.

Falnes, J (2002). *Ocean waves and oscillating systems. Linear interactions including wave-energy extraction*, Cambridge University Press, Cambridge, UK.

Falnes, J (2007). "A review of wave-energy extraction", *Marine Structures*, Vol 20, No 4, pp 185-201.

Fluent (2006), *Fluent 6.3 User's Guide*, Fluent Inc, USA.

Hirt, CW, Nichols, BD (1981). "Volume of fluid (VoF) method for the dynamics of free boundaries", *J. Comp. Phys.*, Vol 39, pp 201-225.

Johns, B (1991). "The modeling of the free surface flow of water over topography", *Coastal Engineering*, Vol 15, pp 257-278.

Lee, CH, Newman, JN, Nielsen, FG (1996). "Wave interactions with an oscillating water column", *Proc 6th Int. Offshore and Polar Eng. Conf.*, ISOPE, Los Angeles, Vol 1, pp 82-90.

LeMéhauté, B (1976). *An Introduction to Hydrodynamics and Water Waves*, Springer-Verlag.

Lopes, MFP, Ricci, P, Gato, LMC, Falcão, AFO (2007). "Experimental and numerical analysis of the oscillating water column inside a surface-piercing vertical cylinder in regular waves". Proc *7th European Wave and Tidal Energy Conference*, Porto, Portugal.

Mittal, S, Tezduyar, TE (1995). “Parallel finite element simulation of 3D incompressible flows— fluid–structure interaction”, *International Journal for Numerical Methods in Fluids*, Vol 21, pp 933–953.

Pontes, MT, Falcão, AFO (2001). “Oceans Energies: Resourses and Utilization”, Proc. *18th World Energy Conference*, Buenos Aires.

Paixão Conde, JM, Gato, LMC (2008). “Numerical study of the air-flow in an oscillating water column wave energy converter”, *Renewable Energy*, Vol 33, No 12, pp 2637-2644.

Paixão Conde, JM, Didier, E (2009). “Numerical simulation of a Oscillating Water Column Wave Energy Converter”, in Portuguese, Proc. *9th Iberoamerican Congress of Mechanical Engineering*, CIBIM9, Las Palmas de Gran Cannaria, Spain.

Panicker, NN (1976). “Power resource estimate of ocean surface waves”, *Ocean Engineering*, Vol 3, No 6, pp 429-439.

Peric, M, Ferziger, JH (1997). *Computational Methods for Fluid Dynamics*, Second edition, Springer.

Ramaswamy, R, Kawahara, M (1987). “Arbitrary lagrangian-eulerian finite element method for unsteady, convective, incompressible viscous free surface fluid flow”, *International Journal for Numerical Methods in Fluids*, Vol 7, pp 1053-1075.

Teixeira, PRF (2001). “Numerical simulation of the compressible and incompressible 3D fluid flow interaction with deformable structures using a finite element method”, in Portuguese, PhD thesis, PPGEC-UFRGS, Porto Alegre, Brazil.

Teixeira, PRF, Awruch, AM (2000). “Numerical simulation of three dimensional incompressible flows using the finite element method”, Proc *8th ENCIT*, Porto Alegre, Brazil.

Teixeira, PRF, Didier, E, Paixão Conde, JM (2009). “Numerical Analysis of OWC wave energy equipment”, in Portuguese, Proc *6th Portuguese Workshops on Coastal and Port Engineering*, Funchal, Portugal.

Wamit (2004). *Wamit manual V.6.2 PC* (www.wamit.com).